Accepted Manuscript

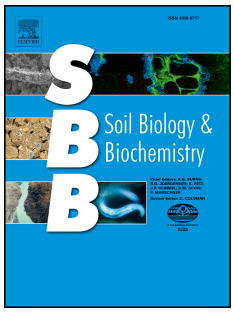

Stoichiometric controls of soil carbon and nitrogen cycling after long-term nitrogen and phosphorus addition in a mesic grassland in South Africa

Per-Marten Schleuss, Meike Widdig, Anna Heintz-Buschart, Alexander Guhr, Sarah Martin, Kevin Kirkman, Marie Spohn

PII: S0038-0717(19)30152-X

DOI: https://doi.org/10.1016/j.soilbio.2019.05.018

Reference: SBB 7497

To appear in: *Soil Biology and Biochemistry*

Received Date: 28 January 2019

Revised Date: 20 May 2019

Accepted Date: 21 May 2019

Please cite this article as: Schleuss, P.-M., Widdig, M., Heintz-Buschart, A., Guhr, A., Martin, S., Kirkman, K., Spohn, M., Stoichiometric controls of soil carbon and nitrogen cycling after long-term nitrogen and phosphorus addition in a mesic grassland in South Africa, *Soil Biology and Biochemistry* (2019), doi: https://doi.org/10.1016/j.soilbio.2019.05.018.

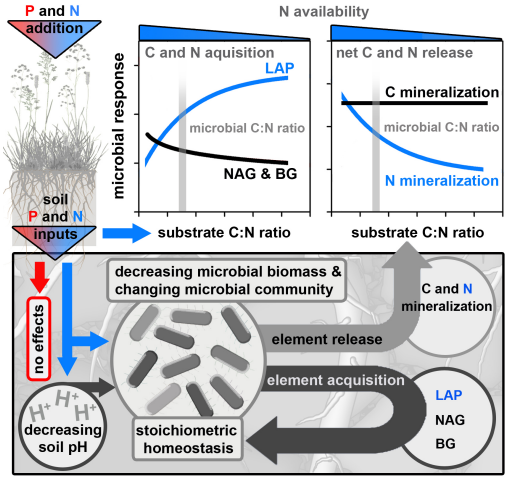

Stoichiometric controls of soil carbon and nitrogen cycling after long-term nitrogen and phosphorus addition in a mesic grassland in South Africa

Per-Marten Schleuss[1*], Meike Widdig[1], Anna Heintz-Buschart[2,3], Alexander Guhr[1], Sarah Martin[1], Kevin Kirkman[4], Marie Spohn[1]

Short-title: Stoichiometric controls of C and N cycling

[1] Department of Soil Biogeochemistry, Soil Biology, Bayreuth Center of Ecology and Environmental Research (BayCEER), University of Bayreuth, Germany

[2] Department of Soil Ecology, UFZ-Helmholtz Centre for Environmental Research, Halle (Saale), Germany

[3] Bioinformatics Unit, German Centre for Integrative Biodiversity Research (iDiv) Halle-Jena-Leipzig

[4] School of Life Sciences, University of KwaZulu-Natal, South Africa

*Corresponding author: Per-Marten Schleuss

e-mail: per.schleuss@uni-bayreuth.de

phone: ++49- (0)921-55-5732

Paper type: Research Article (Regular Paper)

Declarations of interest: None

Key words: N and P fertilization, C:N stoichiometry, C and N release, C and N acquisition, microbial respiration, enzyme activity, pH effect, microbial community composition, DNA-sequencing

Abstract

Terrestrial ecosystems have experienced rising nitrogen (N) inputs during the last decades with consequences for belowground carbon (C) and N dynamics. This study investigates how long-term N and phosphorus (P) additions affect microbial community composition, and to what extent microbial homeostasis explains changes in different processes involved in soil C and N cycling in response to nutrient addition. We studied a 66-year-old nutrient addition experiment in a mesic grassland in South Africa, consisting of four different levels of N addition (0, 7, 14, and 21 g N m^{-2} yr^{-1}) with and without P addition (0, and 9 g P m^{-2} yr^{-1}). Despite strong changes in the microbial community (observed through 16S rRNA gene and ITS amplicon sequencing), the microbial biomass C:N ratio did not change. N addition decreased microbial N acquisition as indicated by reduced leucine-aminopeptidase activity, and increased microbial net N mineralization. In contrast, predicted relative abundances of functional genes involved in degradation of labile C compounds (e.g. cellulose, hemicellulose, and chitin) as well as β-glucosidase and N-acetylglucosaminidase activities increased with elevated N availability. In combination, this pointed to a more intensive investment of microorganisms into C acquisition upon N addition. In contrast, N addition and associated soil acidification decreased microbial biomass and respiration and altered the community composition with prokaryotes being more affected than fungi. Nitrogen addition increased the relative abundance of gram-positive over gram-negative bacteria and favored taxa with low genome-size. Taken together, our findings support the concept that C and N cycling processes can be explained by the property of the soil microbial community to keep the element ratio of its biomass constant and by its reaction to soil acidification. Our findings suggest that predicted elevated N inputs might largely shape soil C and N cycling because the soil microbial community adjusts metabolic processes, which allows it to maintain its biomass stoichiometry constant.

1. Introduction

Grassland ecosystems worldwide have received increasing amounts of nitrogen (N) and phosphorous (P) due to anthropogenic activities during the last decades (Vitousek et al., 1997; Vitousek et al., 2010). Especially N inputs due to atmospheric deposition and fertilizer application have strongly increased, while P inputs are much lower (Penuelas et al., 2013). High N inputs have changed the availability of N in soil leading to an increase in aboveground net primary productivity (ANPP) (LeBauer and Treseder, 2008), and changes in plant species composition in many grasslands (Wedin and Tilman, 1996; Clark and Tilman, 2008). Changes in nutrient inputs affect the C:N:P ratios of soil and the availability of N and P, and it is expected, that stoichiometric deviations between the substrate and the microbial community might be one major factor controlling microbial processes of C and N cycling (Spohn, 2016). The reason for this is that the soil microbial community is homeostatic, i.e., it maintains its C:N:P ratio within a small range (Xu et al., 2013; Cleveland and Liptzin, 2007). According to the concept of consumer-driven nutrient recycling, soil carbon (C) and N cycling is largely controlled by microbial element demand and supply (Sterner and Elser, 2002; Zechmeister-Boltenstern et al., 2015). Soil microorganisms are expected to maintain their element stoichiometry in the way that they (a) acquire and immobilize missing nutrients, (b) adjust element turnover times by keeping scarce elements in the biomass for a longer period of time or (c) release elements present in excess with respect to the microbial demand (Mooshammer et al., 2014; Spohn, 2016). In this study, we use the term “acquisition” when referring to processes of C and N mobilization. Further, we use the term “release” to describe the production of CO_2 and inorganic N ($NH_4^+ + NO_3^-$) over time.

Many studies have shown that N addition directly and indirectly leads to changes in the microbial community composition (Bradley et al., 2006; Ramirez et al., 2010; Fierer et al., 2012; Ramirez et al., 2012) and affects processes of microbial C and N cycling. Furthermore,

N addition has often been shown to decrease soil microbial biomass and reduces C mineralization rates (Treseder, 2008; Janssens et al., 2010; Liu and Greaver, 2010; Yan et al., 2010; Ramirez et al., 2012), which might have different reasons. First, high inorganic N concentrations can inhibit oxidative enzymes, thereby lowering the decomposition of organic matter (Carreiro et al., 2000; Sinsabaugh et al., 2005; Sinsabaugh, 2010). Second, elevated N addition can reduce microbial N mining (Moorhead and Sinsabaugh, 2006; Craine et al., 2007; Ramirez et al., 2012) and lower microbial overflow respiration (Manzoni et al., 2012; Spohn, 2015).

Nitrogen addition was also reported to indirectly affect the soil microbial community and functioning, in the way that changed plant species composition and changed primary productivity shift the microbial community through altered soil C inputs (Bardgett et al., 1999; Liu and Greaver, 2010; Lange et al., 2015; Ramirez et al., 2010; Lange et al., 2015). Accordingly, Leff et al. (2015) demonstrated that microbial community shifts were strongly associated with changes in plant species composition across 25 grassland ecosystems. Other studies have shown that N addition leads to soil acidification, which reduces soil microbial biomass, changes microbial community composition, decreases bacterial and fungal growth rates and thereby strongly reduces soil respiration (Treseder, 2008; Rousk et al., 2009). For instance, Rousk et al. (2011) demonstrated declining bacterial and increasing fungal growth rates due to a strong decrease in soil pH after 150 years of N addition. This finding is in line with De Vries et al. (2006) who demonstrated that N addition decreased the fungi-to-bacteria ratio through declining soil pH values.

While C mineralization tends to decrease with N addition, net N mineralization (gross N mineralization minus microbial N immobilization) usually increases with elevated N addition in forest (Andersson et al., 2001; Vestgarden et al., 2003; Le Nave et al., 2009) and in grassland soils (Ma et al., 2011; Zhang et al., 2012). Whether mineralization or immobilization prevails depends on the substrate C:N ratio, as net N mineralization has been

shown to increase with decreasing litter C:N ratios (Manzoni et al., 2008; Heuck and Spohn, 2016).

In this study, we aimed to understand to what extent the property of the soil microbial community to maintain its biomass element ratio constant (stoichiometric homeostasis) explains soil C and N cycling processes. For this purpose, we studied a 66-year-old nutrient addition experiment consisting of four different levels of N addition with and without P addition in a mesic grassland in South Africa. We hypothesized that long-term N addition (and to a lesser extent P addition) decreases the soil microbial biomass, changes the prokaryotic and fungal community, but does not shift the microbial biomass C:N ratio (Hypothesis 1). Further, we expected that N addition changes microbial processes of C and N acquisition and release in the way that due to N addition microbes invest more into C acquisition and release less C, and invest less into N acquisition and release more N. Specifically, this means that C mineralization rates were hypothesized to decrease, and labile C-degrading enzymes (e.g. β-glucosidase and N-acetylglucosaminidase activities) were expected to increase upon N addition (Hypothesis 2). In addition, N mineralization rates were hypothesized to increase, while leucine-aminopeptidase activity was hypothesized to decrease with N addition (Hypothesis 3).

2. Material and Methods

2.1. Study area

The long-term nutrient addition experiment is located in a mesic grassland savanna near Pietermaritzburg, KwaZulu-Natal, South Africa (29° 24´E, 30° 25´S). The experimental site (covering about 5000 m^2) is placed on top of a slightly south-east facing slope (840 m a.s.l.). Mean annual precipitation amounts to 790 mm, and most of the rainfall occurs during October to April (Tsvuura and Kirkman, 2013). The mean annual temperature is 18°C and monthly minimum and maximum temperature range between 8.8 °C and 26.4 °C (Fynn et al., 2003, Ward et al., 2017). The vegetation is classified as a southern tall grassland (Ward et al., 2017)

that is interspersed with C3-trees (e.g. *Acacia sieberiana*) (Fynn and O'connor, 2005). However, no trees were present in the experimental area. The savanna grassland is characterized by high plant diversity with up to 14 different grass species and 9 different forb species per square meter (Zeglin et al., 2007). Predominant C4 grass species are *Themeda triandra*, *Heteropogon contortus* and *Tristachya leucothrix*. The ANPP is strongly controlled by water availability and approximately reaches 300 g m^{-2} yr^{-1} (Fynn and O'connor, 2005). Aboveground biomass is regularly removed at the end of the vegetation period, while fires have been prevented since the beginning of the experiment. The soil is shallow (0.6 – 1 m) and has a loamy clay texture (5% sand, 46% silt, 49% clay), moderate acidic pH value (pH in H_2O: 5.5) and high stocks of total organic C (TOC, 7.3 kg C m^{-2}) and total N (TN, 0.47 kg N m^{-2}) in the upper 15 cm. According to the world reference base (WRB) the soil is classified as Acrisol, and has been evolved on shales of the Karoo sedimentary sequence (Fynn et al., 2003).

2.2. Experimental set-up

The nutrient addition experiment was established in 1951 by the University of KwaZulu-Natal and has been maintained since then. In total, 24 plots (each 9 m x 2.7 m) were sampled, which are randomly arranged in a block design with a distance of 1 m to each other. The experiment includes four different levels of N addition with and without P addition. In total, this amounts to eight different treatments with respective N and P addition rates provided in Table 1. Each treatment is replicated three times. Nitrogen has been supplied annually in solid form as limestone ammonium-nitrate (28% N) and P has been supplied annually in solid form as super-phosphate (10.5% P). Soil samples were taken at the end of the vegetation period in February in 2017. Six soil cores were taken from the upper 15 cm at each plot and combined into one mixed sample. In addition, a small soil profile was prepared and undisturbed soil cores (100 cm^3) were taken from the upper 15 cm to determine soil bulk density. All soil

samples were transferred in field-moist conditions to the University of Bayreuth within one week after sampling.

2.3. Soil and microbial analyses:

Sample preparation: Field-moist soil samples were sieved (<2 mm) and roots were removed. For analysis of element concentrations, soil material was dried at 50 °C and subsequently milled. Soil water content and water holding capacity (WHC) were analyzed gravimetrically. For determination of WHC, fresh samples were oversaturated with water, placed on a sand bath for 24 hours until field capacity (100% WHC) was reached, and then dried at 105°C. Soil samples were adjusted to a WHC of 60% and incubated at 15°C for seven weeks in order to determine C and net N mineralization.

Element concentrations in soil and soil-water extracts: Total organic C (TOC) and total N (TN) concentrations were analyzed using an elemental analyzer (Vario Max Elementar, Hanau, Germany). Soil pH of air-dried soil was measured in a ratio (v/v) of 1.0 to 2.5 in distilled water (pH_{H2O}).

A dry-mass equivalent of 20 g soil was extracted in 80 ml distilled water and filtered (0.45µm). Total dissolved nitrogen (DN; TOC-TN Analyser, Jena Analytics) and dissolved organic carbon (DOC; TOC-TN Analyser, Jena Analytics) in the water extracts were determined.

Net N mineralization: Net N mineralization rates were determined in soil water extracts according to Heuck et al. (2018) assuming negligible effects of NH_4^+ adsorption to soil particles or organic matter (Haney et al., 2006). Net N mineralization rates were calculated based on the linear increase in the $N\text{-}NH_4^+$ plus $N\text{-}NO_3^-$ concentration in soil over time. For this purpose, we prepared soil-water extracts at day 0, 7, 14, 21, 35, and 49 of the incubation. Sub-samples of 20 g soil dry-mass equivalent were extracted in 80 ml distilled water on an overhead shaker for one hour. The water extracts were filtered (0.45 µm) by means of an under-pressure device and subsequently measured for NH_4^+ via flow injection analysis (FIA-

Lab, MLE Dresden) and NO_3 via ion chromatography (Metrohm 881 Compact IC pro, Metrohm Switzerland). The N mineralization rate was calculated as the increase in inorganic N over time.

C mineralization: CO_2 was measured continuously (every 2 hours) from 10 g soil dry-mass equivalents incubated at 15°C over a period of 60 days using a respirometer (Respicond V, Nordgen Innovations) (Heuck and Spohn, 2016). C mineralization rates were calculated based on the linear increase in CO_2-C over time.

Microbial C and N: Microbial biomass C and N concentrations (MBC and MBN) were determined using the chloroform fumigation-extraction method (Brookes et al., 1982; Vance et al., 1987). Fumigated samples (incubated for 1 day in the dark) and non-fumigated samples were extracted in 0.5 M K_2SO_4 in a ratio of 1:5 (soil:extractant). After filtration, the samples were diluted in a ratio of 1:20, and dissolved C and N were measured using a TOC/TN Analyzer (multi N/C 2100, Analytik Jena, Jena, Germany). For calculating microbial biomass C and N, the concentration of the non-fumigated sample was subtracted from the one of the fumigated sample and multiplied by a conversion factor of 2.22 (Jenkinson, 2004).

Microbial community: The V4 region of the prokaryotic 16S rRNA gene and the ITS2 region of fungal rRNA operons were amplified and sequenced on a MiSeq (Illumina) sequencer (see Supplementary Material for details). After removal of the primer sequences, reads were quality-filtered and clustered at maximum resolution using the DADA2 workflow (Callahan *et al.* 2016). Taxonomy was assigned to the resultant, non-chimeric sequences representing operational taxonomic units (OTUs) using the bayesian classifier implemented in mothur (Schloss et al. 2009) against the UNITE v7.2 database for ITS (Kõljalg et al. 2013), and the SILVA v128 database for 16S sequences (Quast et al., 2012), before fungal functional classes were assigned using FunGuild (Nguyen *et al.* 2016) and prokaryotic functions were predicted using PanFP (Jun et al., 2015). Gram staining characteristics and genome sizes were assigned to genera, based on the NCBI attributes collected in http://www-ab2.informatik.uni-

tuebingen.de/megan/taxonomy/microbialattributes.zip and literature searches (Huson et al., 2007).

Enzyme activities: Soil enzymes of β-1,4-glucosidase (BG), β-1,4-N-acetylglucosaminidase (NAG), and leucine-aminopeptidase (LAP) were determined using the fluorogenic substrates, 4-methylumbelliferyl-β-D-glucoside, 4-methylumbelliferyl-N-acetyl-β-D-glucosaminide and L-leucine-7-amino-4-methylcoumarine according to German et al. (2011) and Herold et al. (2014). One gram of moist soil was homogenized in 50 ml of sterile water by shaking for 20 min. The soil homogenates were pipetted into microplates and 100 µl of 1 mM fluorescent substrate solution was added. Samples were preincubated in the dark at 15°C for 30 min, and subsequently measured fluorometrically after 0, 30, 60, and 180 min using a microplate reader (Infinite® 200 PRO, TECAN). Fluorescence was corrected for quenching of the soil as well as for the fluorescence of substrate and soil (German et al., 2011). Enzyme activity was calculated from the slope of net fluorescence over incubation time in nmol g^{-1} h^{-1} according to German et al. (2011).

2.4. Statistics

Statistical analyses were carried out using SigmaPlot 13 (SYSSTAT) and R version 3.3 (R Development Core Team). Simple regressions were used to identify relationships between response variables. All regressions were considered significant at $p < 0.05$.

We implemented two-way ANOVAs with N addition as first factor and P addition as second factor to identify single and interacting effects between N and P addition. However, two-way ANOVA revealed hardly any interactions between N and P addition, and showed N addition to be the predominant factor controlling microbial characteristics and rates of C and N cycling (Supplementary Material, Table 1). Therefore, we additionally used mixed linear models (MLM) to calculate independent effects of N and (P) addition using the “nlme” package and the “multcomp” package for post-hoc tests in R. For this purpose, treatments were grouped according to their N and P addition rates. Additional variance, resulting from non-target

parameters, was eliminated by selecting either N or P as random factor. Further, MLM regressions were used to analyze to what extent DN and pH explain variance in microbial biomass, whereby variance of one parameter was eliminated by selecting the other (DN or pH) as random factor (the random factors were consistently classified with n=8 as follows: pH classes <4.5, 4.6-5.0, >5.1; DN classes 0-20, 20-40 and >40 mg DN kg soil^{-1}). Before applying two-way ANOVA and MLM, data were checked for normality and homogeneity of variance and transformed if necessary.

We applied structural equation modeling (SEM) using the "lavaan" package for R. SEM is a robust multivariate statistical approach allowing for hypotheses testing of complex path-relation networks (Grace et al., 2010; Eisenhauer et al., 2015). It was used to test causal relationships between N addition and microbial biomass, C mineralization, C and N availabilities (measured as DN and DOC concentrations), substrate stoichiometry (measured as DOC:DN ratio), and soil acidification (measured as soil pH). The model fit was evaluated using Root Mean Square Error of Approximation (RMSEA), chi square (χ^2), and the p value of χ^2. Note that a high p value of χ^2 (> 0.05) indicates a good model fit as it significantly differs from the baseline model.

Metabarcoding based data were analyzed in R. Beta-diversity was visualized using NMDS of Jensen-Shannon divergences (JSD) of community profiles at OTU level (using vegan, phyloseq and ade4 packages). N and P addition were assessed as drivers of beta-diversity by permutational multivariate analysis of variance of JSDs (using adonis2 of the vegan package). The same analysis was conducted at taxonomic ranks such as genus, family, order and class level, and using weighted UniFrac distances for prokaryotic data (using vegan and phyloseq packages). In addition, the soil measurements with the strongest additional and independent explanatory values were determined using forward selection, also using permutational multivariate analyses. Simpson's diversity index and Pielou's evenness were calculated after rarefaction to equal read numbers (using vegan). Effective genome size was determined as the

means of genome sizes of the observed genera weighted by the relative abundance of the genera in each sample. Microbial taxa that were affected by N and/or P addition were identified using DESeq2, with a model employing N addition levels, P addition and their interaction as fixed effects. For the predicted relative gene abundances based on microbial community abundances, multivariate association with linear models (using MaAsLin) was performed for N and P addition. Gene abundances were considered significantly associated with either factor, if FDR-values < 0.01 were observed.

3. Results

3.1. Changes in element concentrations

The TN concentration amounted to 3.0 g N kg soil^{-1} and the TOC concentration to 47 g C kg soil^{-1} in the control. Thus, 0.47 kg N m^{-2} and 7.3 kg C m^{-2} were stored in the upper 15 cm of the soil. Even though high amounts of N have been added throughout the last 66 years, the TOC and TN concentrations did not differ significantly between the control and nutrient addition treatments (Table 1). However, N addition strongly raised the concentration of DN. Dissolved N concentrations were 6.3 mg N kg soil^{-1} in the control and were 5.6, 6.7, and 20.6 times higher in the low, medium, and high N addition level without P addition, respectively. P addition significantly reduced DN concentrations in the low, medium and high N level as compared to corresponding single N levels. In the NP treatments, DN concentrations gradually increased with increasing N addition rate (Table 1). The increase in DOC concentration in response to N addition, however, was less strong, and only significant differences occurred in the N treatments without P addition. Here, the DOC concentrations in the low N level without P addition significantly differed from that of the highest N level without P addition. Single P addition and combined NP additions had no effect on DOC concentrations (Table 1). The soil pH decreased with increasing N addition rate, and was more than one unit lower in the highest N level without P addition (pH:4.1) than in the control (pH: 5.4). P addition did not significantly affect the soil pH (Table 1).

3.2. Soil microbial biomass and stoichiometry

MBC concentrations ranged between 380 and 960 mg C kg soil^{-1} across all treatments, and the highest values were found in the control. MBC decreased significantly with intensified N addition (Fig. 1a). It was 0.79, 0.65, and 0.48 times lower in the low, medium, and high N addition treatment than in the sites without N addition, respectively. Phosphorus addition did not significantly change MBC (Supplement Material, Table S1). MBC showed a negative linear correlation with DN ($R^2 = 0.67$, $p < 0.001$), a positive asymptotic relationship with the DOC:DN ratio ($R^2 = 0.85$, $p < 0.001$), a positive linear relationship with the TOC:TN ratio, and positive linear correlation with soil pH ($R^2 = 0.68$, $p < 0.00$) (Fig. S1 a-d). Mixed linear models revealed that DN and pH independently contributed to explain variance of MBC (DN: $R^2 = 0.63$, $p < 0.001$; pH: $R^2 = 0.36$, $p < 0.001$). The microbial biomass was homeostatic with respect to its C:N ratio (mean microbial biomass C:N: 7.8; Fig. 1b), despite strong changes in the dissolved organic matter (DOM) C:N ratios with increasing N addition (Table 1), and strong changes in the microbial community composition (see chapter 3.3.).

3.3. Microbial community changes

Long-term N and P addition induced changes in microbial community composition (Fig. 2a). We observed significant effects of N and P addition for both the prokaryotic and fungal community (Supplementary Material, Table S2). However, N addition affected community compositions more strongly than P addition, especially in the prokaryotic community. Next to N addition, pH was found to best explain the shifts in prokaryotic community composition (Fig. 2b). Both N and P addition contributed to the observed shift in the fungal community, with additional explanatory power of DIP and DOC:DN ratio (Fig. 2b). The effect of pH on the fungal community was only significant if N and P addition were not considered in the model (explaining 20% of the observed variance, Supplementary Material, Table S3).

Differences in community composition through single and combined N and P addition were observable at all studied taxonomic ranks (OTUs, genera, families, orders, classes and phyla

(for prokaryotes) and divisions (for fungi) (Supplementary Material, Table S4). We found that within the prokaryotic community especially gram-positive bacteria increased with N addition (mostly Actinobacteria) as well as some gram-negative bacteria, which are known to be associated with low pH (e.g. Acidobacteria subgroup 13, Supplementary Material, Table S4). Within the fungal community, a relatively decrease in Basidiomycota with N addition was observable, which is noteworthy as this group includes the majority of all ectomycorrhizal species (Supplementary Material, Table S4). However, we did not observe any significant changes in predicted fungal functional classes with N addition.

Predicted changes in Gram$^+$:Gram$^-$ ratio and effective genome size

For prokaryotic communities, a clear asymptotic increase in gram-positive relative to gram-negative bacteria was observed with intensified N addition, and an exponential decrease with DOC:DN ratio (Supplementary Material, Fig. S2a-b). The relative increase in gram-positive bacteria was accompanied by an increase in abundance of bacteria with smaller genome sizes at higher N addition levels. Effective genome size was 0.95, 0.88, and 0.78 times lower than that of the sites without N addition in the low, medium and high N addition levels, respectively (Supplementary Material, Fig. S2c). Moreover, the effective genome size was strongly related to the DOC:DN ratio with a remarkable decrease once the substrate C:N ratio was below the microbial biomass C:N ratio (Supplementary Material, Fig. S2d).

Predicted abundance of labile C degrading enzymes

The abundance of genes encoding hydrolytic enzymes targeting cellulose, hemicellulose, and chitin was predicted to increase with higher N addition rate (Fig. 3). Moreover, the predicted relative abundances of genes encoding hemicellulose, cellulose, and chitin degrading enzymes showed positive linear correlations with the DN concentration (Fig. 4a-c). Further, they decreased exponentially with the DOC:DN ratio (Fig. 4d-f), and linearly with the TOC:TN ratio (Fig. 4g-i) and with increasing soil pH (Fig. 4j-l). In contrast, the predicted relative gene abundance of oxidative enzymes targeting more complex compounds (e.g. the phenol-oxidase

gene abundances that catalyze lignin degradation) decreased with N addition (Fig. 3). The predicted relative abundance of the lignin-degrading phenol-oxidase decreased linearly with DN concentration, increased asymptotically with the DOC:DN ratio, and increased linearly with soil pH (Supplementary Material, Fig. S3).

3.4. Hydrolytic enzyme activities

Results of predicted relative abundances of genes encoding hydrolytic enzymes concurred with measurements of hydrolytic enzyme activities. Leucine-aminopeptidase activity per unit soil decreased with increasing N addition rate. It was significantly lower in the soil of the medium (0.4 times) and high N addition treatment (0.28 times) than in the soil without N addition (Fig. 5a). In contrast, P addition caused no effect on leucine-aminopeptidase activity (Supplementary Material, Table S1). Leucine-aminopeptidase activity per unit soil decreased exponentially with DN concentrations, increased asymptotically with DOC:DN ratio, and increased linearly with the TOC:TN ratio as well as exponentially with soil pH (Supplementary Material, Fig. S4a-d). Further, we found that the leucine-aminopeptidase activity per unit MBC strongly decreased once the C:N ratio of the DOM approached the C:N ratio of the microbial biomass (Fig. 5b).

The β-glucosidase activity per unit soil did not significantly differ between N addition levels (Fig. 5c) and P addition levels (Supplementary Material, Table S1). However, β-glucosidase activity per unit MBC decreased exponentially once the DOC:DN ratio approximated that of the microbial biomass (Fig. 5d). Very similar patterns were observed for the N-acetylglucosaminidase activity. N-acetylglucosaminidase activity per unit soil did not significantly differ between N addition levels (Fig. 5e) and P addition levels (Supplementary Material, Table S1), while N-acetylglucosaminidase activity per unit MBC exponentially decreased with the DOC:DN ratio (Fig. 5f). Both β-glucosidase and N-acetylglucosaminidase activities per unit soil tended to increase with DN concentration, decreased with the DOC:DN

ratio, and increased with the TOC:TN ratio as well as with soil pH, although most correlations were only marginally significant ($p = 0.07$) (Supplementary Material, Fig. S4e-l).

3.5. C mineralization rate

C mineralization ranged between 5.4 and 11.5 mg C kg soil^{-1} day^{-1} across all treatments. It was not affected by P addition (Supplementary Material, Table 1), but gradually declined with increasing N addition rate (Fig 6a). C mineralization was significantly lower in the medium (0.70 times) and the highest N level (0.52 times) compared to the sites without N addition. It decreased exponentially with DN concentrations ($R^2 = 0.33$, $p = 0.005$), increased asymptotically with DOC:DN ratios ($R^2 = 0.44$, $p < 0.001$), and linearly with theTOC:TN ratio ($R^2 = 0.37$, $p = 0.002$) as well as with soil pH ($R^2 = 0.50$, $p < 0.001$), and MBC ($R^2 = 0.47$, $p < 0.001$) (Supplementary Material, Fig. S5a-d). Further, we found that below a critical C:N ratio of 10.4, C mineralization almost ceased. However, when C mineralization rates were based on unit MBC, no significant linear correlations between C mineralization and DN ($R^2= 0.02$; $p = 0.64$), TOC:TN ratio ($R^2= 0.01$; $p = 0.87$), soil pH ($R^2= 0.02$; $p = 0.50$) or DOC:DN ratio ($R^2 = 0.02$; $p = 0.49$; Fig. 6b) were observed.

Structural equation modeling showed that N addition directly constrained C mineralization, and indirectly affected soil pH with negative feedbacks on C mineralization rates. Further, N addition significantly affected DN and DOC concentrations as well as the DOC:DN ratio, which together impaired the microbial biomass pool. In total, the combined factors explained 59% of the variance of C mineralization and 91% of the variance of MBC. Surprisingly, the model did not indicate a direct effect of MBC on C mineralization (Fig. 7).

3.6. Net N mineralization rate

Net N mineralization was about 10 times lower than C mineralization and ranged between 0.04 and 0.65 mg N kg soil^{-1} day^{-1} across all treatments. It gradually increased with N addition rate, and was 4.0, 4.7, and 6.7 times higher in the low, medium and high N treatment, respectively, compared to the sites without N addition (Fig. 6c). Net N mineralization rates

increased asymptotically with DN concentrations (R^2 = 0.33, p = 0.005), decreased exponentially with higher DOC:DN ratio (R^2 = 0.44, p < 0.001), and showed a negative linear relationship with the TOC:TN ratio (R^2 = 0.27, p = 0.009) as well as with soil pH (R^2 = 0.44, p < 0.001) (Supplementary Material, Fig. S6e-h). We identified the critical threshold soil TOC:TN ratio for net N mineralization to be 19.5, which is the intercept with the x axis (Heuck et al., 2016). Above this ratio, net N mineralization was almost zero, indicating that N immobilization leveled out gross N mineralization. Net N mineralization per MBC showed a negative exponential relationship with the DOC:DN ratio, indicating that N mineralization is strongly increased if the C:N ratio of the DOM was close to the microbial biomass C:N ratio (Fig. 6d).

4. Discussion

4.1. Microbial homeostasis as a driver of C and N cycling

While microbial biomass strongly decreased with N addition, the C:N ratio of soil microbial biomass did not differ significantly between the treatments despite high annual N and P inputs for several decades. Previous studies did not find consistent results with respect to effects of nutrient addition or changing element availabilities on microbial biomass stoichiometry. While some studies indicated a change in the C:N ratio of the microbial biomass (Hu et al., 2010; Li et al., 2012; Khan and Joergensen, 2019), other studies demonstrated that the microbial community maintains its C:N ratio independent of nutrient availabilities (Joergensen and Scheu 1999; Heuck et al. 2015; Tapia-Torres et al. 2015). The latter is in line with our observation and supports the concept of microbial homeostasis (Cleveland and Liptzin, 2007; Xu et al., 2013; Spohn, 2016), and is especially noteworthy, given that the microbial community structure and function shifted due to N addition (see chapter 4.4.). The reason why the microbial community was able to maintain its biomass stoichiometry despite strong changes in element availabilities in its environment is very likely that it adjusted the rates of processes of C and N cycling according to its stoichiometric demands.

4.2. Stoichiometric controls of C and N acquisition

Nitrogen addition caused a marked decline in leucine-aminopeptidase activity per unit soil, indicating that microbes reduce their investment into N acquisition from organic pools once microbial N demands are saturated (Saiya-Cork et al., 2002; Nemergut et al., 2008; Ramirez et al., 2012). This agrees with other studies reporting decreased gross N mineralization in forest and grasslands due to N fertilizer application (Corre et al., 2003; Hoeft et al., 2014). Contrarily, β-glucosidase and N-acetylglucosaminidase activities per unit soil as well as predicted relative gene abundances of labile C degrading enzymes tended to increase with N addition rate. This indicates that microbes invest more energy into C acquisition when provided with high loads of inorganic N, as shown previously (Carreiro et al., 2000; Allison and Vitousek, 2005; Zeglin et al., 2007). Increased β-glucosidase and N-acetylglucosaminidase activities likely render organic C available, which balances the high N availability. Our interpretation that C and N cycling in soil is driven by stoichiometric homeostasis of the soil microbial biomass was especially supported by the relationship between the DOC:DN ratio and β-glucosidase as well as N-acetylglucosaminidase activities. The strong decrease in leucine-aminopeptidase activity and the increase in β-glucosidase and N-acetylglucosaminidase activities at DOC:DN ratios < 8 indicate that microbes stop investing into N acquisition while promoting C acquisition if the C:N ratio of the DOM is smaller than the C:N ratio of the microbial biomass. The reason for this is that DOM forms the dominant substrate on which soil microorganisms thrive (Marschner and Kalbitz, 2003) and its C:N ratio determines whether N is scarce or sufficient with respect to microbial demands.

4.3. Controls on net N and C release

Net N mineralization gradually increased with N addition, which is in line with previous studies on grassland and forest soils (Le Nave et al., 2009; Ma et al., 2011; Zhang et al., 2012). Especially once the substrate C:N ratio converged to that of the microbial biomass, net

N mineralization increased substantially. This was even more apparent when the net N mineralization rate was based on MBC. The most plausible explanation for this is that microbes released large amounts of N, when the substrate N exceeds the microbial N demand (Manzoni et al., 2008; Heuck and Spohn, 2016), while they strongly immobilize N when thriving on N poor substrate. The threshold element ratio for net N mineralization observed here indicates that above a soil C:N ratio of 19 and above a DOC:DN ratio of 23, N immobilization balanced gross N mineralization leading to a strong reduction of net N release. This is in accordance with previously reported threshold C:N ratios for net N mineralization in litter (Kaiser et al., 2014; Heuck and Spohn, 2016).

In contrast to increasing N mineralization rates, C mineralization decreased with higher N availability, as similarly shown for other grassland and forest soils (Söderström et al., 1983; Berg and Matzner, 1997; Magill and Aber, 1998; Hagedorn et al., 2003; Sjöberg et al., 2003; Craine et al., 2007; Ramirez et al., 2012; Spohn et al., 2016). However, we found no clear relationship between C mineralization per unit MBC and TOC, TN, DN, DOC or DIN concentrations or their ratios. This indicates that reduced overflow respiration or decreased N mining (Craine et al., 2007; Manzoni et al., 2012) in this mesic grassland potentially contributed less to the decreased C mineralization under elevated N. Therefore, we could not explicitly confirm our second hypothesis postulating that C mineralization decreases due to stoichiometric constraints.

SEM showed that C mineralization was reduced mainly due to N addition and reduced soil pH. The most plausible explanation for this is that increased N availability and decreased pH caused by high N addition rates reduced the microbial biomass pool. Further, it is likely that N addition and associated soil acidification inhibited the production and activity of oxidative enzymes that are involved in the depolymerization of complex organic substances (e.g. lignin) (Frey et al., 2004; Gallo et al., 2004; Sinsabaugh et al., 2005). In agreement with this, we

found that the predicted gene abundance of phenol-oxidase was reduced through N addition and associated soil acidification.

4.4. N addition changes microbial community composition

Long-term N addition decreased the microbial biomass and changed the microbial community composition. One explanation for this could be that N addition imbalanced the availability of C relative to N (Chen et al., 2018). Increasing N addition caused a shift towards bacteria with a lower genome size, which mostly belong to the gram-positive bacteria (e.g. Mycobacterium sp.) or in some cases to gram-negative bacteria (e.g. Acidobacterium sp.) that are well adapted to low soil pH (Eichorst et al., 2011). The bacterial groups with lower genome size can be expected to be more efficient in C acquisition and uptake because they can cope more easily with imbalances between C and N. First, a reduction of the genome size goes along with reduced amounts of C tied up in DNA and mRNA per cell (Cottrell and Kirchman, 2016). Second, many of these bacterial groups are specialists for degradation of specific substrates with small but well adapted enzyme sets (Martínez-Núñez et al., 2013). Since fungi are in general equipped with a larger set of enzymes than bacteria, targeting multiple polysaccharides (Berlemont, 2017), it is likely that they can compensate more easily for stoichiometric imbalances in their environment. This might explain why the fungal community changed less strongly than the prokaryotic community in response to nutrient inputs to soil.

Another explanation could be that N addition decreased soil pH, which constrained the functioning of the microbial community and thereby affected the pool sizes and community composition of soil microorganisms. This is in agreement with Rousk et al, (2010) who pointed out that bacteria have a very narrow pH optimum for growth tolerance, likely as a consequence of high aluminum concentration below pH of 5 (Pietri and Brookes 2008; Rousk et al. 2009) and lower C solubility with decreasing soil pH (Andersson et al. 2000). The low soil pH in the soils that have received high amounts of N was likely induced by nitrification

processes that release protons by oxidizing ammonium to nitrate. For bacteria, we observed that N addition increased the relative abundance of groups that are known to be associated with low pH (e.g. Acidobacteria subgroup 13, Firmicutes) and reduced the relative abundances of groups associated with neutral or higher pH (e.g. Acidobacteria subgroups 5 and 17, Nitrospira, Anaerolineae, Chloroflexia) (Bartram et al., 2014). However, the fungal community was less strongly affected by N inputs than the prokaryotic community, likely because their physiological traits make them more resistant to a reduced soil pH. This is consistent with previous studies indicating that fungi respond less sensitively towards soil acidification than bacteria (Vries et al., 2006; Zhang et al., 2008; Rousk et al., 2009; Rousk et al., 2010). Reasons for this could be that saprotrophic fungi have thick cell walls with crosslinked polymers (Madigan et al., 2017), and thus are less vulnerable to changes in soil pH as compared to bacteria (Madigan et al., 2017). Moreover, filamentous fungi can extend their hyphal networks over long distances (Posada et al., 2012) and can transport nutrients, which means that they can mitigate stoichiometric imbalances.

5. Conclusions

Despite high N addition to soil over many decades, the microbial biomass C:N ratio did not change in this grassland. This is especially noteworthy given that the microbial biomass decreased, and the community of fungi and, in particular, of prokaryotes was strongly altered. Thus, the microbial community was able to maintain its stoichiometry by adjusting processes of C and N cycling. A higher N availability likely enhanced microbial investments into C acquisition as indicated by an increase of β-glucosidase and N-acetylglucosaminidase activities, and a predicted increase in labile C degrading prokaryotic taxa. In contrast, leucine-aminopeptidase activity decreased due to N addition, suggesting that the microbial community invested less into N acquisition under high N inputs. Yet, the decrease in C mineralization in response to N addition can be attributed to a decrease in pH rather than to stoichiometric constraints. While N strongly affected processes of the C and N cycle, P

addition did not change soil C and N cycling. In conclusion, our results suggest that changes in the rates of C and N cycling processes can largely be explained (1) by the property of the soil microbial community to adjust processes of element cycling to element availabilities and maintain its biomass stoichiometry and (2) by its reaction to soil acidification when exposed to high addition of N over long periods.

Acknowledgements

We thank Renate Krauss, Uwe Hell, and Karin Söllner for technical assistance. We thank the chemical analytics (CAN) of the Bayreuth Center of Ecological and Environmental Research (BayCEER) for performing parts of the chemical analyses and Beatrix Schnabel of the Helmholtz-Centre for Environmental Research (UFZ) for sequencing. The study was funded by the German Research Foundation within the Emmy Noether program (grant SP1389/6-1). Anna Heintz-Buschart was funded by the German Centre for Integrative Biodiversity Research (iDiv) Halle-Jena-Leipzig of the German Research Foundation (FZT 118). The scientific results have in part been computed at the High-Performance Computing (HPC) Cluster EVE, a joint effort of both the Helmholtz Centre for Environmental Research - UFZ and the German Centre for Integrative Biodiversity Research (iDiv) Halle-Jena-Leipzig.

Figure Captions

Figure 1: Microbial biomass carbon (MBC) **(a)** and molar microbial biomass C:N ratio as a function of N addition rate. Red dots show means ± SD (n=6), whereby treatments receiving N and treatments with combined N and P addition were grouped together. Mixed linear models were applied to indicate effects of N addition. The variance derived from P addition was eliminated selecting it as random factor. Significant differences are indicated by lower case letters ($p < 0.05$). Correlations were considered significant at $p < 0.05$ (n=24).

Figure 2: Fungal and prokaryotic community composition depending on N and P addition **(a)** and explained variance of microbial community compositions by measured soil parameters **(b)**. Microbial OTU community composition was analyzed using ITS and 16S amplicon sequencing. For panel **(a)**: Data are represented via non-metric multi-dimensional scaling of Jensen-Shannon divergence (JSD) between taxonomic profiles. For panel **(b)**: Soil parameters were tested by forward selection using permutational multivariate analysis of variance based on JSD of microbial communities at OTU level.

Figure 3: Predicted relative gene abundances of selected C degrading exoenzymes depending on N and P addition. (Hemi)cellulose degrading enzymes include beta-glucosidase, endo-1,4-beta-xylanase, endoglucanase, 1,4-beta-D-glucan cellobiohydrolase; Chitin-degrading enzymes include endo-beta-N-acetylglucosaminidase, chitinase; Lignin-degrading enzyme include phenol-monooxidase. Annotations are taken from the Kyoto Encyclopedia of Genes and Genomes (KEGG): K01179= endoglucanase; K01225= cellulose 1,4-beta-cellobiosidase; K05349= beta-glucosidase (bglX); K05350= beta-glucosidase (bglB); K01181= endo-1,4-beta-xylanase; K01227= mannosyl-glycoprotein endo-beta-N-acetylglucosaminidase; K01183= chitinase; K00505= tyrosinas.

Figure 4: Correlations between predicted relative gene abundances of hemicellulose, cellulose, chitin degrading with dissolved N (DN) **(a-c)**, DOC:DN ratio **(d-e)**, TOC:TN ratio **(f-h)**, and soil pH **(i-k)**. Predicted hemicellulose degrading enzymes: beta-glucosidase, endo-1,4-beta-xylanase; predicted cellulose degrading enzymes: endoglucanase, 1,4-beta-D-glucan cellobiohydrolase; predicted chitin-degrading enzymes: endo-beta-N-acetylglucosaminidase, chitinase. For DN one value was deemed as outlier, and was not included.

Figure 5: Activity of leucine-aminopeptidase, β-glucosidase and N-acetylglucosaminidase depending on N addition rate **(a, c, e)** and the enzyme activity per unit microbial biomass carbon (MBC) as a function of the DOC:DN ratio **(b, d, f)**. Red dots show means ± SD (n = 6); N and NP treatments were grouped together. Mixed linear models were applied to indicate effects of N addition. The variance derived from P addition was eliminated selecting it as random factor. Significant differences ($p < 0.05$) are indicated by lower-case letters. For all panels correlations were considered significant at $p < 0.05$ (n=24).

Figure 6: Net C and N mineralization rates depending on N addition rate **(a, c)**, and net C and N mineralization per unit microbial biomass carbon (MBC) (qC*min* and qN*min*) as a function of the DOC:DN ratio **(b,d)**. For panel **(a)** and **(b)**: Red dots show means ± SD (n = 6); N and NP treatments were grouped together. Mixed linear models were applied to indicate effects of N addition. The variance derived from P addition was eliminated selecting it as random factor. Significant differences ($p < 0.05$) are indicated with small letters. For all panels correlations were deemed significant at $p < 0.05$ (n=24).

Figure 7: Pathway-model predicting effects of N addition on microbial biomass carbon (MBC) and C mineralization. The initial model included all pathways that are represented here (arrows). Significant paths are illustrated by bold arrows with standardized path coefficients, whereby positive path coefficients illustrate a positive relationship and *vice versa*. Numbers in red boxes state the explained variance of each factor. The model was evaluated using Chi square (χ^2), Comparative Fit Index (CFI), Tucker Lewis Index (TLI), and Root Mean Square error of Approximation (RMSEA). Note that CFI and TLI were close to one, RMSEA was < 0.05, and the high p value of χ^2 all together indicated a good model fit.

583 ## *References*

584 Allison, S.D., Vitousek, P.M., 2005. Responses of extracellular enzymes to simple and complex
585 nutrient inputs. Soil Biology and Biochemistry 37, 937–944.

586 Andersson, P., Berggren, D., Johnsson, L., 2001. 30 Years of N Fertilisation in a Forest Ecosystem-The
587 Fate of Added N and Effects on N Fluxes. Water, air, and soil pollution 130, 637–642.

588 Andersson, Stefan; Nilsson, S. Ingvar; Saetre, Peter (2000): Leaching of dissolved organic carbon
589 (DOC) and dissolved organic nitrogen (DON) in mor humus as affected by temperature and pH. In
590 *Soil Biology and Biochemistry* 32 (1), pp. 1–10.

591 Bardgett, R.D., Mawdsley, J.L., Edwards, S., Hobbs, P.J., Rodwell, J.S., Davies, W.J., 1999. Plant species
592 and nitrogen effects on soil biological properties of temperate upland grasslands. Functional
593 Ecology 13, 650–660.

594 Bartram, A.K., Jiang, X., Lynch, M.D.J., Masella, A.P., Nicol, G.W., Dushoff, J., Neufeld, J.D., 2014.
595 Exploring links between pH and bacterial community composition in soils from the Craibstone
596 Experimental Farm. FEMS Microbiology Ecology 87, 403–415.

597 Berg, B., Matzner, E., 1997. Effect of N deposition on decomposition of plant litter and soil organic
598 matter in forest systems. Environmental Reviews 5, 1–25.

599 Berlemont, R., 2017. Distribution and diversity of enzymes for polysaccharide degradation in fungi.
600 Scientific reports 7, 222.

601 Bradley, K., Drijber, R.A., Knops, J., 2006. Increased N availability in grassland soils modifies their
602 microbial communities and decreases the abundance of arbuscular mycorrhizal fungi. Soil Biology
603 and Biochemistry 38, 1583–1595.

604 Brookes, P.C., Powlson, D.S., Jenkinson, D.S., 1982. Measurement of microbial biomass phosphorus in
605 soil. Soil Biology and Biochemistry 14, 319–329.

606 Carreiro, M.M., Sinsabaugh, R.L., Repert, D.A., Parkhurst, D.F., 2000. Microbial enzyme shifts explain
607 litter decay responses to simulated nitrogen deposition. Ecology 81, 2359–2365.

608 Chen, H., Li, D., Zhao, J., Zhang, W., Xiao, K., Wang, K., 2018. Nitrogen addition aggravates microbial
609 carbon limitation: Evidence from ecoenzymatic stoichiometry. Geoderma 329, 61–64.
610 Clark, C.M., Tilman, D., 2008. Loss of plant species after chronic low-level nitrogen deposition to
611 prairie grasslands. Nature 451, 712.
612 Cleveland, C.C., Liptzin, D., 2007. C: N: P stoichiometry in soil: is there a "Redfield ratio" for the
613 microbial biomass? Biogeochemistry 85, 235–252.
614 Corre, M.D., Beese, F.O., Brumme, R., 2003. Soil nitrogen cycle in high nitrogen deposition forest:
615 changes under nitrogen saturation and liming. Ecological applications 13, 287–298.
616 Cottrell, M.T., Kirchman, D.L., 2016. Transcriptional control in marine copiotrophic and oligotrophic
617 bacteria with streamlined genomes. Applied and Environmental Microbiology, AEM-01299.
618 Craine, J.M., Morrow, C., Fierer, N., 2007. Microbial nitrogen limitation increases decomposition.
619 Ecology 88, 2105–2113.
620 De Vries, F.T. de, Hoffland, E., van Eekeren, N., Brussaard, L., Bloem, J., 2006. Fungal/bacterial ratios
621 in grasslands with contrasting nitrogen management. Soil Biology and Biochemistry 38, 2092–
622 2103.
623 Eichorst, S.A., Kuske, C.R., Schmidt, T.M., 2011. Influence of plant polymers on the distribution and
624 cultivation of bacteria in the phylum Acidobacteria. Applied and Environmental Microbiology 77,
625 586–596.
626 Eisenhauer, N., Bowker, M.A., Grace, J.B., Powell, J.R., 2015. From patterns to causal understanding:
627 structural equation modeling (SEM) in soil ecology. Pedobiologia 58, 65–72.
628 Fierer, N., Lauber, C.L., Ramirez, K.S., Zaneveld, J., Bradford, M.A., Knight, R., 2012. Comparative
629 metagenomic, phylogenetic and physiological analyses of soil microbial communities across
630 nitrogen gradients. The ISME journal 6, 1007.
631 Frey, S.D., Knorr, M., Parrent, J.L., Simpson, R.T., 2004. Chronic nitrogen enrichment affects the
632 structure and function of the soil microbial community in temperate hardwood and pine forests.
633 Forest Ecology and Management 196, 159–171.

634 Fynn, R.W.S., Haynes, R.J., O'connor, T.G., 2003. Burning causes long-term changes in soil organic
635 matter content of a South African grassland. Soil Biology and Biochemistry 35, 677–687.
636 Fynn, R.W.S., O'connor, T.G., 2005. Determinants of community organization of a South African
637 mesic grassland. Journal of Vegetation Science 16, 93–102.
638 Gallo, M., Amonette, R., Lauber, C., Sinsabaugh, R.L., Zak, 2004. Microbial community structure and
639 oxidative enzyme activity in nitrogen-amended north temperate forest soils. Microbial ecology
640 48, 218–229.
641 German, D.P., Weintraub, M.N., Grandy, A.S., Lauber, C.L., Rinkes, Z.L., Allison, S.D., 2011.
642 Optimization of hydrolytic and oxidative enzyme methods for ecosystem studies. Soil Biology and
643 Biochemistry 43, 1387–1397.
644 Grace, J.B., Anderson, T.M., Olff, H., Scheiner, S.M., 2010. On the specification of structural equation
645 models for ecological systems. Ecological Monographs 80, 67–87.
646 Hagedorn, F., Spinnler, D., Siegwolf, R., 2003. Increased N deposition retards mineralization of old soil
647 organic matter. Soil Biology and Biochemistry 35, 1683–1692.
648 Haney, R.L., Haney, E.B., Hossner, L.R., Arnold, J.G., 2006. Development of a new soil extractant for
649 simultaneous phosphorus, ammonium, and nitrate analysis. Communications in Soil Science and
650 Plant Analysis 37, 1511–1523.
651 Herold, N., Schöning, I., Berner, D., Haslwimmer, H., Kandeler, E., Michalzik, B., Schrumpf, M., 2014.
652 Vertical gradients of potential enzyme activities in soil profiles of European beech, Norway spruce
653 and Scots pine dominated forest sites. Pedobiologia 57, 181–189.
654 Heuck, Christine; Weig, Alfons; Spohn, Marie (2015): Soil microbial biomass C: N: P stoichiometry and
655 microbial use of organic phosphorus. In *Soil Biology and Biochemistry* 85, pp. 119–129.
656 Heuck, C., Spohn, M., 2016. Carbon, nitrogen and phosphorus net mineralization in organic horizons
657 of temperate forests: stoichiometry and relations to organic matter quality. Biogeochemistry 131,
658 229–242.

659 Heuck, C., Smolka, G., Whalen, E.D., Frey, S., Gundersen, P., Moldan, F., Fernandez, I.J., Spohn, M.,
660 2018. Effects of long-term nitrogen addition on phosphorus cycling in organic soil horizons of
661 temperate forests. Biogeochemistry 141, 167–181.
662 Hoeft, I., Keuter, A., Quiñones, C.M., Schmidt-Walter, P., Veldkamp, E., Corre, M.D., 2014. Nitrogen
663 retention efficiency and nitrogen losses of a managed and phytodiverse temperate grassland.
664 Basic and Applied Ecology 15, 207–218.
665 Hu, Y.-L., Zeng, D.-H., Liu, Y.-X., Zhang, Y.-L., Chen, Z.-H., Wang, Z.-Q., 2010. Responses of soil
666 chemical and biological properties to nitrogen addition in a Dahurian larch plantation in
667 Northeast China. Plant and soil 333, 81–92.
668 Huson, D.H., Auch, A.F., Qi, J., Schuster, S.C., 2007. MEGAN analysis of metagenomic data. Genome
669 research 17, 377–386.
670 Janssens, I.A., Dieleman, W., Luyssaert, S., Subke, J.-A., Reichstein, M., Ceulemans, R., Ciais, P.,
671 Dolman, A.J., Grace, J., Matteucci, G., 2010. Reduction of forest soil respiration in response to
672 nitrogen deposition. Nature geoscience 3, 315.
673 Jenkinson, D., 2004. Measuring soil microbial biomass. Soil Biology and Biochemistry 36, 5–7.
674 Joergensen, R.G., Scheu, S., 1999. Response of soil microorganisms to the addition of carbon,
675 nitrogen and phosphorus in a forest Rendzina. Soil Biology and Biochemistry 31, 859–866.
676 Jun, S.-R., Robeson, M.S., Hauser, L.J., Schadt, C.W., Gorin, A.A., 2015. PanFP: pangenome-based
677 functional profiles for microbial communities. BMC research notes 8, 479.
678 Kaiser, C., Franklin, O., Dieckmann, U., Richter, A., 2014. Microbial community dynamics alleviate
679 stoichiometric constraints during litter decay. Ecology letters 17, 680–690.
680 Khan, K.S., Joergensen, R.G., 2019. Stoichiometry of the soil microbial biomass in response to
681 amendments with varying C/N/P/S ratios. Biology and Fertility of Soils, 1–10.
682 Lange, M., Eisenhauer, N., Sierra, C.A., Bessler, H., Engels, C., Griffiths, R.I., Mellado-Vázquez, P.G.,
683 Malik, A.A., Roy, J., Scheu, S., 2015. Plant diversity increases soil microbial activity and soil carbon
684 storage. Nature communications 6, 6707.

Le Nave, Vance, E.D., Swanston, C.W., Curtis, P.S., 2009. Impacts of elevated N inputs on north temperate forest soil C storage, C/N, and net N-mineralization. Geoderma 153, 231–240.

LeBauer, D.S., Treseder, K.K., 2008. Nitrogen limitation of net primary productivity in terrestrial ecosystems is globally distributed. Ecology 89, 371–379.

Leff, J.W., Jones, S.E., Prober, S.M., Barberán, A., Borer, E.T., Firn, J.L., Harpole, W.S., Hobbie, S.E., Hofmockel, K.S., Knops, J.M.H., 2015. Consistent responses of soil microbial communities to elevated nutrient inputs in grasslands across the globe. Proceedings of the National Academy of Sciences 112, 10967–10972.

Li, Y., Wu, J., Liu, S., Shen, J., Huang, D., Su, Y., Wei, W., Syers, J.K., 2012. Is the C: N: P stoichiometry in soil and soil microbial biomass related to the landscape and land use in southern subtropical China? Global biogeochemical cycles 26.

Liu, L., Greaver, T.L., 2010. A global perspective on belowground carbon dynamics under nitrogen enrichment. Ecology letters 13, 819–828.

Ma, L.-N., Lü, X.-T., Liu, Y., Guo, J.-X., Zhang, N.-Y., Yang, J.-Q., Wang, R.-Z., 2011. The effects of warming and nitrogen addition on soil nitrogen cycling in a temperate grassland, northeastern China. Plos One 6, e27645.

Madigan, M.T., Martinko, J.M., Parker, J., 2017. Brock biology of microorganisms. Pearson.

Magill, A.H., Aber, J.D., 1998. Long-term effects of experimental nitrogen additions on foliar litter decay and humus formation in forest ecosystems. Plant and soil 203, 301–311.

Manzoni, S., Jackson, R.B., Trofymow, J.A., Porporato, A., 2008. The global stoichiometry of litter nitrogen mineralization. Science 321, 684–686.

Manzoni, S., Taylor, P., Richter, A., Porporato, A., Ågren, G.I., 2012. Environmental and stoichiometric controls on microbial carbon-use efficiency in soils. New Phytologist 196, 79–91.

Marschner, B., Kalbitz, K., 2003. Controls of bioavailability and biodegradability of dissolved organic matter in soils. Geoderma 113, 211–235.

710 Martínez-Núñez, M.A., Poot-Hernandez, A.C., Rodríguez-Vázquez, K., Perez-Rueda, E., 2013.
711 Increments and duplication events of enzymes and transcription factors influence metabolic and
712 regulatory diversity in prokaryotes. Plos One 8, e69707.
713 Moorhead, D.L., Sinsabaugh, R.L., 2006. A theoretical model of litter decay and microbial interaction.
714 Ecological Monographs 76, 151–174.
715 Mooshammer, M., Wanek, W., Zechmeister-Boltenstern, S., Richter, A.A., 2014. Stoichiometric
716 imbalances between terrestrial decomposer communities and their resources: mechanisms and
717 implications of microbial adaptations to their resources. Frontiers in microbiology 5, 22.
718 Nemergut, D.R., Townsend, A.R., Sattin, S.R., Freeman, K.R., Fierer, N., Neff, J.C., Bowman, W.D.,
719 Schadt, C.W., Weintraub, M.N., Schmidt, S.K., 2008. The effects of chronic nitrogen fertilization
720 on alpine tundra soil microbial communities: implications for carbon and nitrogen cycling.
721 Environmental Microbiology 10, 3093–3105.
722 Penuelas, J., Poulter, B., Sardans, J., Ciais, P., van der Velde, M., Bopp, L., Boucher, O., Godderis, Y.,
723 Hinsinger, P., Llusia, J., 2013. Human-induced nitrogen–phosphorus imbalances alter natural and
724 managed ecosystems across the globe. Nature communications 4, 2934.
725 Pietri, J. AciegoC; Brookes, P. C. (2008): Relationships between soil pH and microbial properties in a
726 UK arable soil. In *Soil Biology and Biochemistry* 40 (7), pp. 1856–1861.
727 Posada, R.H., Madriñan, S., Rivera, E.-L., 2012. Relationships between the litter colonization by
728 saprotrophic and arbuscular mycorrhizal fungi with depth in a tropical forest. Fungal biology 116,
729 747–755.
730 Quast, C., Pruesse, E., Yilmaz, P., Gerken, J., Schweer, T., Yarza, P., Peplies, J., Glöckner, F.O., 2012.
731 The SILVA ribosomal RNA gene database project: improved data processing and web-based tools.
732 Nucleic acids research 41, D590-D596.
733 Ramirez, K.S., Craine, J.M., Fierer, N., 2012. Consistent effects of nitrogen amendments on soil
734 microbial communities and processes across biomes. Global Change Biology 18, 1918–1927.

735 Ramirez, K.S., Lauber, C.L., Knight, R., Bradford, M.A., Fierer, N., 2010. Consistent effects of nitrogen
736 fertilization on soil bacterial communities in contrasting systems. Ecology 91, 3463–3470.
737 Rousk, J., Bååth, E., Brookes, P.C., Lauber, C.L., Lozupone, C., Caporaso, J.G., Knight, R., Fierer, N.,
738 2010. Soil bacterial and fungal communities across a pH gradient in an arable soil. The ISME
739 journal 4, 1340.
740 Rousk, J., Brookes, P.C., Bååth, E., 2009. Contrasting soil pH effects on fungal and bacterial growth
741 suggest functional redundancy in carbon mineralization. Applied and Environmental Microbiology
742 75, 1589–1596.
743 Rousk, J., Brookes, P.C., Bååth, E., 2011. Fungal and bacterial growth responses to N fertilization and
744 pH in the 150-year 'Park Grass' UK grassland experiment. FEMS Microbiology Ecology 76, 89–99.
745 Saiya-Cork, K.R., Sinsabaugh, R.L., Zak, 2002. The effects of long term nitrogen deposition on
746 extracellular enzyme activity in an Acer saccharum forest soil. Soil Biology and Biochemistry 34,
747 1309–1315.
748 Sinsabaugh, R.L., 2010. Phenol oxidase, peroxidase and organic matter dynamics of soil. Soil Biology
749 and Biochemistry 42, 391–404.
750 Sinsabaugh, R.L., Gallo, M.E., Lauber, C., Waldrop, M.P., Zak, D.R., 2005. Extracellular enzyme
751 activities and soil organic matter dynamics for northern hardwood forests receiving simulated
752 nitrogen deposition. Biogeochemistry 75, 201–215.
753 Sjöberg, G., Bergkvist, B., Berggren, D., Nilsson, S.I., 2003. Long-term N addition effects on the C
754 mineralization and DOC production in mor humus under spruce. Soil Biology and Biochemistry
755 35, 1305–1315.
756 Söderström, B., Bååth, E., Lundgren, B., 1983. Decrease in soil microbial activity and biomasses owing
757 to nitrogen amendments. Canadian Journal of Microbiology 29, 1500–1506.
758 Spohn, M., 2015. Microbial respiration per unit microbial biomass depends on litter layer carbon-to-
759 nitrogen ratio. Biogeosciences 12, 817–823.

760 Spohn, M., 2016. Element cycling as driven by stoichiometric homeostasis of soil microorganisms.
761 Basic and Applied Ecology 17, 471–478.
762 Spohn, M., Pötsch, E.M., Eichorst, S.A., Woebken, D., Wanek, W., Richter, A., 2016. Soil microbial
763 carbon use efficiency and biomass turnover in a long-term fertilization experiment in a temperate
764 grassland. Soil Biology and Biochemistry 97, 168–175.
765 Sterner, R.W., Elser, J.J., 2002. Ecological stoichiometry: the biology of elements from molecules to
766 the biosphere. Princeton University Press.
767 Tapia-Torres, Y., Elser, J.J., Souza, V., García-Oliva, F., 2015. Ecoenzymatic stoichiometry at the
768 extremes: How microbes cope in an ultra-oligotrophic desert soil. Soil Biology and Biochemistry
769 87, 34–42.
770 Treseder, K.K., 2008. Nitrogen additions and microbial biomass: A meta-analysis of ecosystem
771 studies. Ecology letters 11, 1111–1120.
772 Tsvuura, Z., Kirkman, K.P., 2013. Yield and species composition of a mesic grassland savanna in South
773 Africa are influenced by long-term nutrient addition. Austral Ecology 38, 959–970.
774 Vance, E.D., Brookes, P.C., Jenkinson, D.S., 1987. An extraction method for measuring soil microbial
775 biomass C. Soil Biology and Biochemistry 19, 703–707.
776 Vestgarden, L.S., Selle, L.T., Stuanes, A.O., 2003. In situ soil nitrogen mineralisation in a Scots pine
777 (Pinus sylvestris L.) stand: effects of increased nitrogen input. Forest Ecology and Management
778 176, 205–216.
779 Vitousek, P.M., Aber, J.D., Howarth, R.W., Likens, G.E., Matson, P.A., Schindler, D.W., Schlesinger,
780 W.H., Tilman, D.G., 1997. Human alteration of the global nitrogen cycle: sources and
781 consequences. Ecological applications 7, 737–750.
782 Vitousek, P.M., Porder, S., Houlton, B.Z., Chadwick, O.A., 2010. Terrestrial phosphorus limitation:
783 mechanisms, implications, and nitrogen–phosphorus interactions. Ecological applications 20, 5–
784 15.

785 Ward, D., Kirkman, K., Tsvuura, Z., 2017. An African grassland responds similarly to long-term
786 fertilization to the Park Grass experiment. Plos One 12, e0177208.
787 Wedin, D.A., Tilman, D., 1996. Influence of nitrogen loading and species composition on the carbon
788 balance of grasslands. Science 274, 1720–1723.
789 Xu, X., Thornton, P.E., Post, W.M., 2013. A global analysis of soil microbial biomass carbon, nitrogen
790 and phosphorus in terrestrial ecosystems. Global Ecology and Biogeography 22, 737–749.
791 Yan, L., Chen, S., Huang, J., Lin, G., 2010. Differential responses of auto-and heterotrophic soil
792 respiration to water and nitrogen addition in a semiarid temperate steppe. Global Change Biology
793 16, 2345–2357.
794 Zechmeister-Boltenstern, S., Keiblinger, K.M., Mooshammer, M., Peñuelas, J., Richter, A., Sardans, J.,
795 Wanek, W., 2015. The application of ecological stoichiometry to plant–microbial–soil organic
796 matter transformations. Ecological Monographs 85, 133–155.
797 Zeglin, L.H., Stursova, M., Sinsabaugh, R.L., Collins, S.L., 2007. Microbial responses to nitrogen
798 addition in three contrasting grassland ecosystems. Oecologia 154, 349–359.
799 Zhang, N., Wan, S., Li, L., Bi, J., Zhao, M., Ma, K., 2008. Impacts of urea N addition on soil microbial
800 community in a semi-arid temperate steppe in northern China. Plant and soil 311, 19–28.
801 Zhang, X., Wang, Q., Gilliam, F.S., Bai, W., Han, X., Li, L., 2012. Effect of nitrogen fertilization on net
802 nitrogen mineralization in a grassland soil, northern China. Grass and forage science 67, 219–230.
803

Table1: Element concentrations in soil and soil water extracts depending on N and P addition

Variable	Two-way ANOVA			Effect of N addition (among groups)				Effects of N and P addition (within groups)							
	N	P	NxP	N_0	N_7	N_{14}	N_{21}	N_0P_0	N_7P_0	$N_{14}P_0$	$N_{21}P_0$	N_0P_9	N_7P_9	$N_{14}P_9$	$N_{21}P_9$
	(significance level)			(significance level)				(without P)				(with P)			
TOC	n.s.	n.s.	n.s.	A	A	A	A	47^{a} ± 3	43^{a} ± 4	45^{a} ± 2	48^{a} ± 3	49^{a} ± 2	47^{a} ± 2	43^{a} ± 1	48^{a} ± 1
TN	n.s.	n.s.	n.s.	A	A	A	A	3.0^{a} ± 0.1	3.2^{a} ± 0.4	3.3^{a} ± 0.2	3.5^{a} ± 0.1	3.4^{a} ± 0.2	3.2^{a} ± 0.3	3.1^{a} ± 0.1	3.5^{a} ± 0.1
DOC	*	n.s.	n.s.	AB	A	AB	B	121^{ab} ± 8	119^{a} ± 2	137^{ab} ± 9	163^{b} ± 47	137^{a} ± 5	131^{a} ± 6	134^{a} ± 16	150^{a} ± 18
DN	***	**	**	A	B	B	C	6.3^{a} ± 1.0	35.3^{b} ± 10.0	42.2^{b} ± 5.4	130.4^{c} ± 69.8	10.4^{a}* ± 1.9	18.2^{b}* ± 5.3	27.7^{b}* ± 5.4	58.5^{c}* ± 8.8
DOC:DN ratio	***	**	**	A	B	B	C	22.8^{a} ± 5.1	4.2^{b} ± 1.3	3.9^{b} ± 0.7	1.7^{c} ± 0.9	15.6^{a} ± 2.0	8.9^{ab}* ± 2.7	5.7^{bc}* ± 0.4	3.0^{c} ± 0.6
DIP	**	***	**	A	AB	B	B	0.1^{a} ± 0.07	0.1^{a} ± 0.03	0.1^{a} ± 0.01	0.1^{a} ± 0.02	4.7^{a}* ± 1.23	2.3^{ab}* ± 1.01	0.6^{c}* ± 0.28	0.8^{bc}* ± 0.48
pH in H_2O	***	n.s.	n.s.	A	AB	B	C	5.4^{a} ± 0.3	4.9^{ab} ± 0.2	4.7^{bc} ± 0.4	4.1^{c} ± 0.3	5.1^{a} ± 0.2	5.1^{a} ± 0.1	4.8^{ab} ± 0.1	4.3^{b} ± 0.2

Shown are means with standard deviations. Separate and combined effects of N and P addition were tested by two-way ANOVA followed by Tuckey post hoc test. Two-way ANOVA indicates effects of N addition, effects of P addition, and interactions of NxP addition (*, $p < 0.05$; **, $p < 0.01$, ***, $p < 0.001$). Capital case letters show significant differences among N levels ($p < 0.05$), and asterisks indicate significant differences among P levels ($p < 0.05$). Lower-case letters indicate significant difference between N addition rates within P groups (with and without P addition). Abbreviations are N addition rate (in g N m^{-2} yr^{-1}), P addition rate (in g P m^{-2} yr^{-1}), total organic C (TOC in g C kg^{-1}), total N (TN in g N kg^{-1}), dissolved organic C (DOC in mg C kg^{-1}), dissolved total N (DN in mg N kg^{-1}), and dissolved inorganic P (DIP in mg P kg^{-1}).

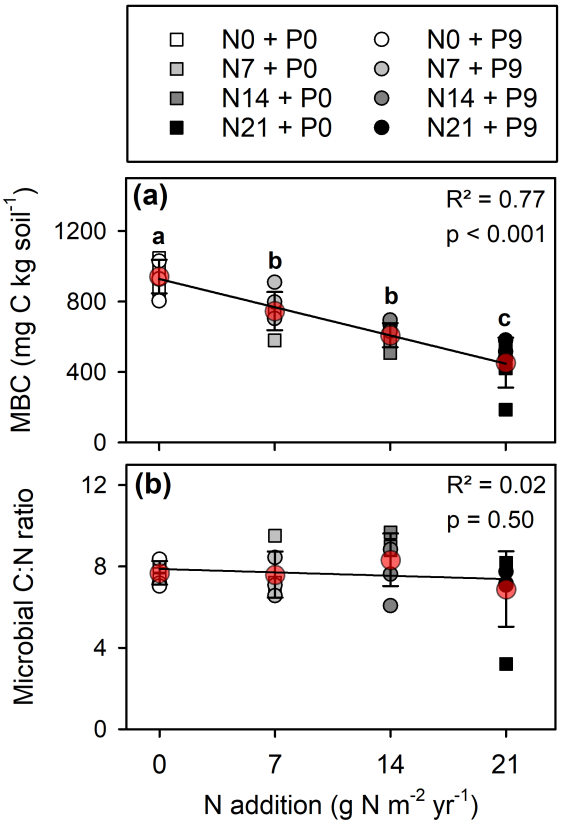

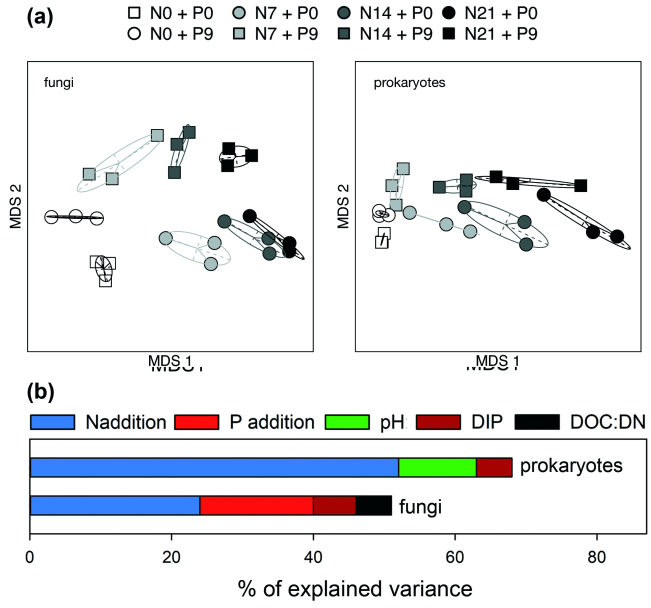

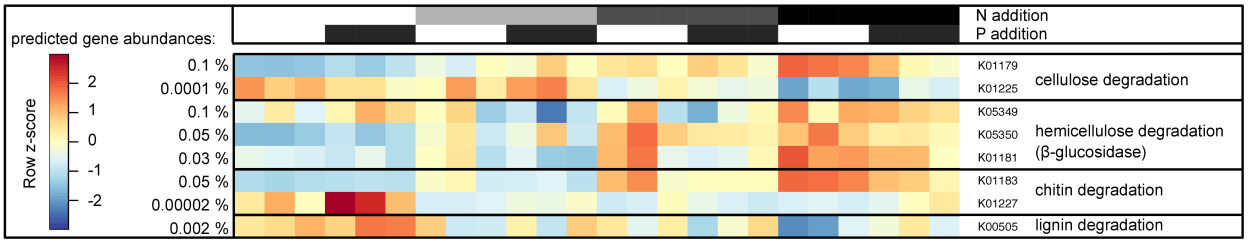

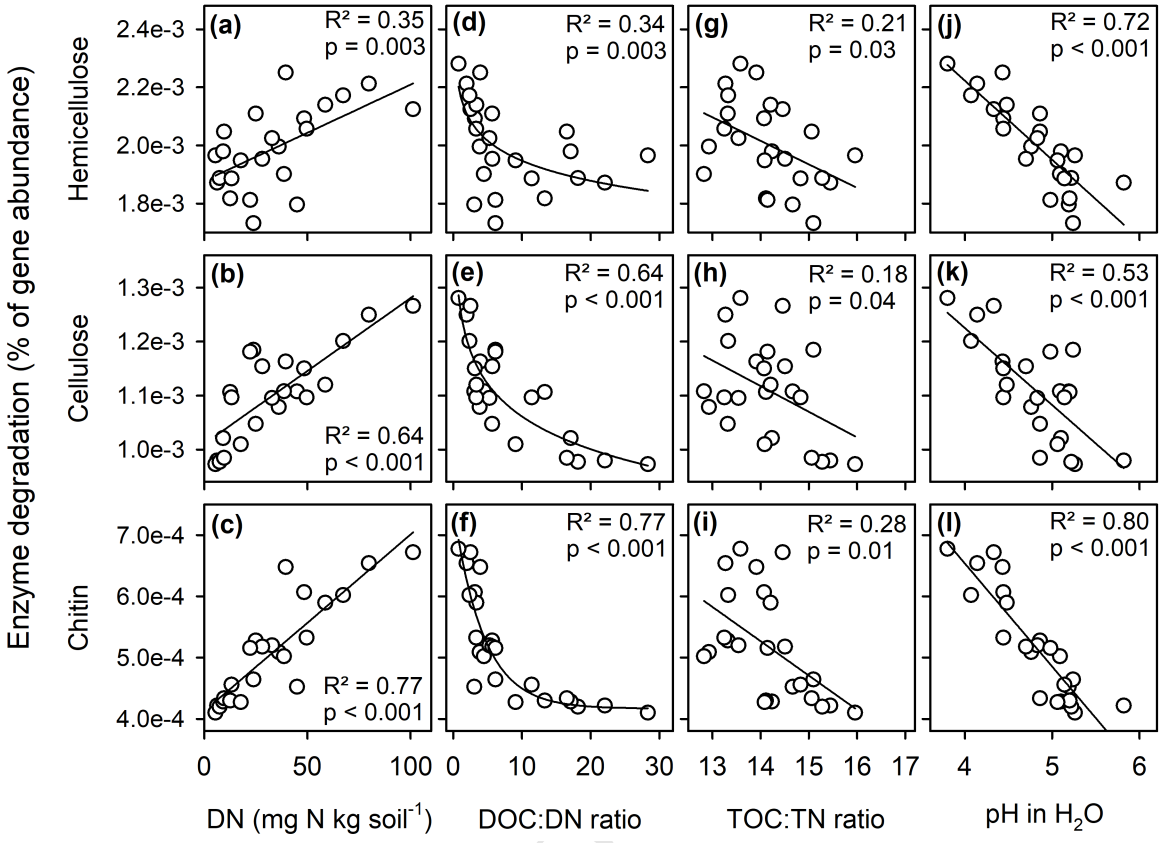
Enzyme degradation (% of gene abundance)
Hemicellulose
Cellulose
Chitin
(a) R² = 0.35 p = 0.003
(b) R² = 0.64 p < 0.001
(c) R² = 0.77 p < 0.001
(d) R² = 0.34 p = 0.003
(e) R² = 0.64 p < 0.001
(f) R² = 0.77 p < 0.001
(g) R² = 0.21 p = 0.03
(h) R² = 0.18 p = 0.04
(i) R² = 0.28 p = 0.01
(j) R² = 0.72 p < 0.001
(k) R² = 0.53 p < 0.001
(l) R² = 0.80 p < 0.001
2.4e-3
2.2e-3
2.0e-3
1.8e-3
1.3e-3
1.2e-3
1.1e-3
1.0e-3
7.0e-4
6.0e-4
5.0e-4
4.0e-4
0 50 100
0 10 20 30
13 14 15 16 17
4 5 6
DN (mg N kg soil-1)
DOC:DN ratio
TOC:TN ratio
pH in H2O

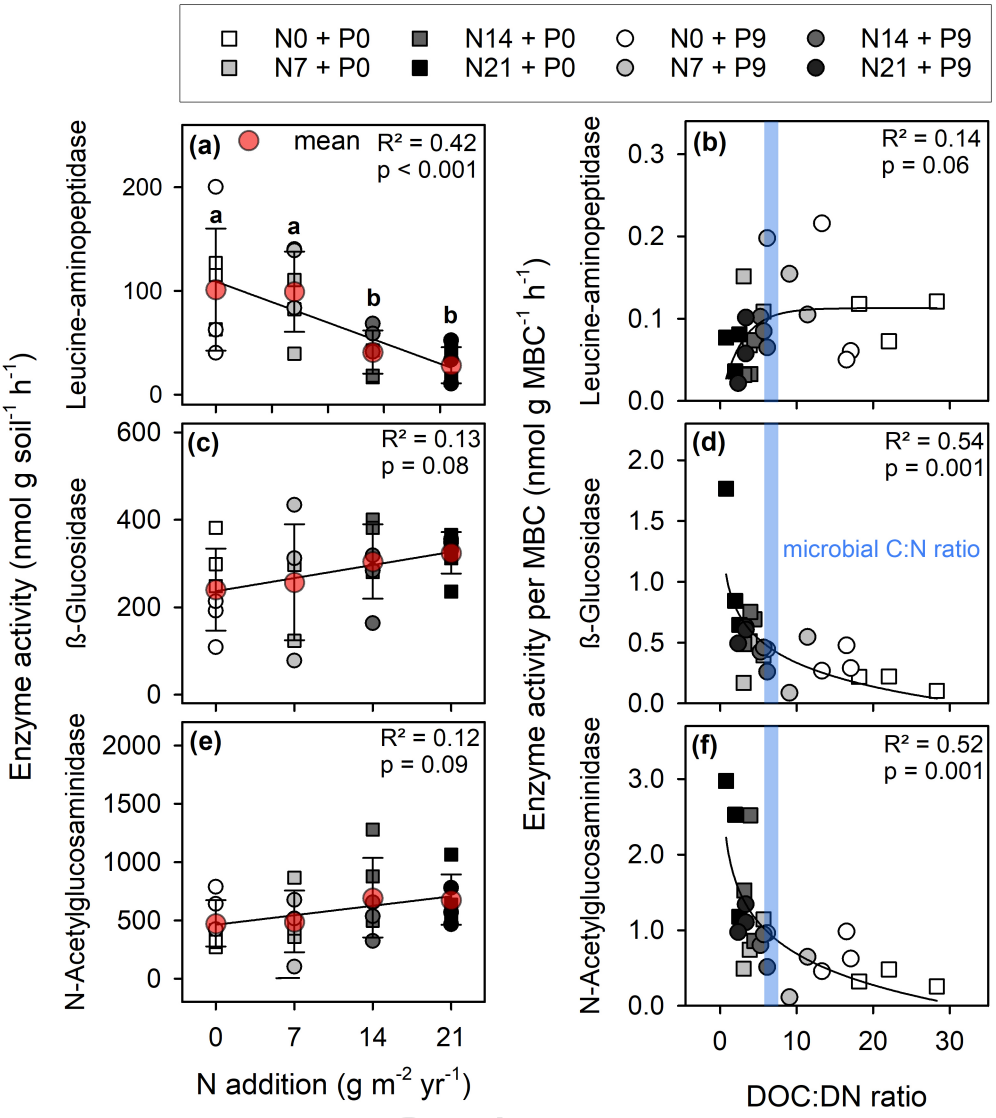
N0 + P0
N7 + P0
N14 + P0
N21 + P0
N0 + P9
N7 + P9
N14 + P9
N21 + P9
(a)
mean
R² = 0.42
p < 0.001
a
a
b
b
(b)
R² = 0.14
p = 0.06
(c)
R² = 0.13
p = 0.08
(d)
R² = 0.54
p = 0.001
microbial C:N ratio
(e)
R² = 0.12
p = 0.09
(f)
R² = 0.52
p = 0.001
Leucine-aminopeptidase
ß-Glucosidase
N-Acetylglucosaminidase
Enzyme activity (nmol g soil-1 h-1)
Enzyme activity per MBC (nmol g MBC-1 h-1)
N addition (g m-2 yr-1)
DOC:DN ratio

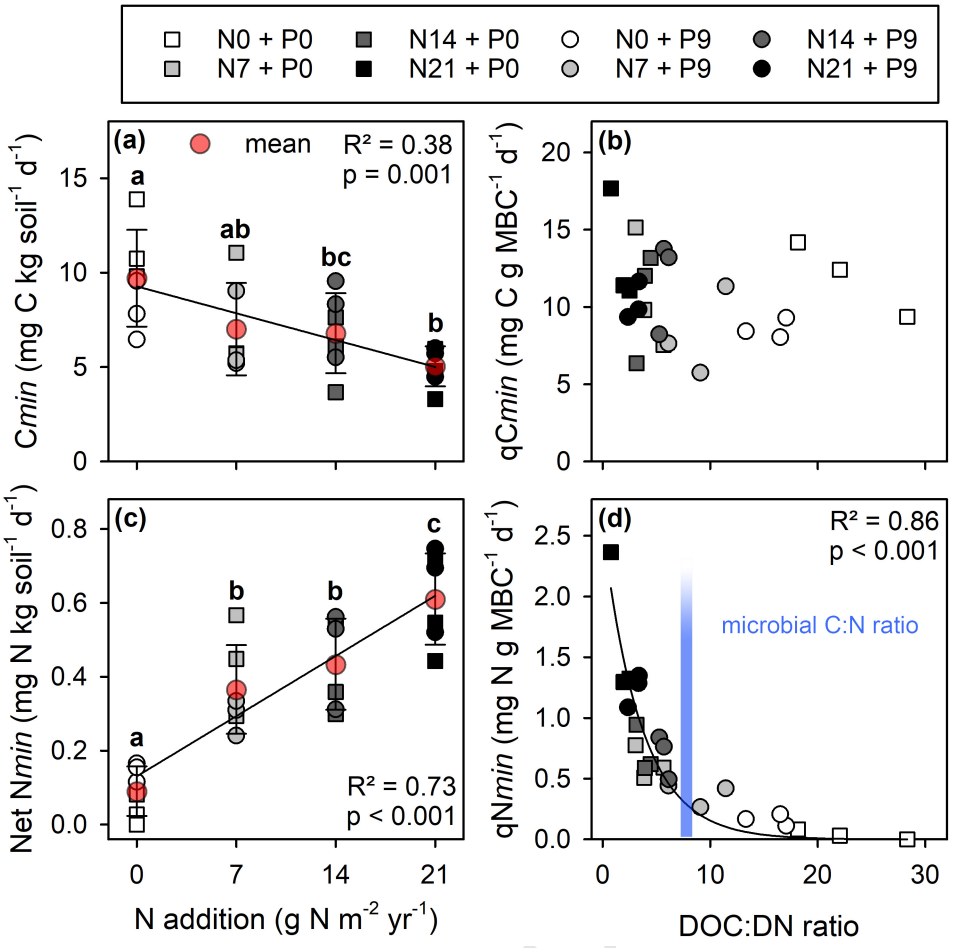

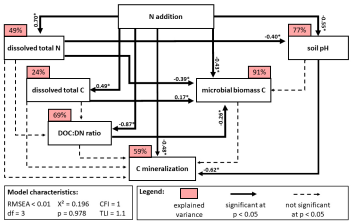

Highlights:

- N (and P) additions affected the microbial community but not their C:N stoichiometry
- Long-term N addition changed processes involved in C and N cycling
- Abundance of genes involved in the C cycle increased with elevated N availability
- Microbes invested less into peptidases and increased net N mineralization
- N addition and associated soil acidification reduced C mineralization rates